PERGAMON

International Journal of Solids and Structures 37 (2000) 887–897

INTERNATIONAL JOURNAL OF SOLIDS and STRUCTURES

www.elsevier.com/locate/ijsolstr

Experimental studies on the temperature fluctuations in deformed thermoplastics with defects

Wenbo Luo[a,*], Tingqing Yang[a], Zhida Li[b], Longwei Yuan[b]

[a]*Department of Mechanics, Huazhong University of Science and Technology, Hubei, 430074, People's Republic of China*
[b]*Institute of Rheological Mechanics, Xiangtan University, Hunan, 411105, People's Republic of China*

Received 22 November 1997; in revised form 7 April 1999

Abstract

The temperature fluctuation during tensile testing of ABS (Acrylonitrile–Butadiene–Styrene), a typical thermoplastic copolymer with prefabricated defects, is experimentally studied in this paper. The initiation and evolution of the local temperature field near the defects are observed with infrared photography. It is shown that the specimen temperature decreases during the initial elastic deformation, whereas it rises in the following inelastic deformation process. According to the experiments, the heat generated from inelastic work is significant and approximates to 25–70 percent of the external work. Based on the microscopic and mesoscopic characteristics of deformation in glassy polymers, a preliminary and qualitative explanation of the cooling and heating phenomena is also presented.

Keywords: Temperature fluctuation; Heat generation; Thermoplastics; Defect

1. Introduction

Because of their importance in industrial applications and their theoretical complications, the mechanical properties and deformation mechanisms of polymers have been extensively studied. Energy changes occur in a deformed glassy polymer due to reorientation, elastic dilatation and plastic deformations. Generally, the major part of the inelastic rate of work contributes to the entropy production, leading to an increase of the local temperature which in turn affects the deformation behavior of the body. Therefore, the mechanical deformation of these materials is accompanied by changes in temperature resulting from the coupled thermomechanical effect.

* Corresponding author.

0020-7683/00/$ - see front matter
PII: S0020-7683(99)00107-9

The early work on thermoelasticity was done by Duhamel (1837), Thomson (1853) and Compton and Webster (1915) for metallic continua. Thereafter, the advances in the study of irreversible thermodynamics (Prigogine, 1962) gave a keen impetus to the developments in the thermomechanical coupling problems of inelastic solids. Dillon (1962a) presented a nonlinear thermoelastic theory. Cernocky and Krempl (1980) proposed a coupled thermoviscoplasticity theory based on the overstress constitutive equation and applied it to investigate special types of loading: pure torsion, uniaxial loading and cyclic loading. Ghoneim (1986, 1990) and Ghoneim and Matsuoka (1987) presented coupled thermoviscoplasticity equations and used them to solve the problems of the dynamic loading of a thick-walled cylinder and the cyclic loading of an end-constrained cylinder. Paglietti (1982) and Audoly and Paglietti (1985) discussed the general equation for the coupled thermo-elastic–plastic phenomena occurring in a cylindrical specimen during a tensile test at a finite strain rate, and stated that heat production due to dissipation of mechanical work could produce strain rate effects. Beginning in 1985, Allen (1985, 1986, 1991) published a series of papers dealing with thermomechanical coupling in viscoplastic uniaxial metallic bars. So far as the thermoviscoelastic coupling models are concerned, initial work was done by Schapery (1969), Christensen (1967, 1971) and Crochet and Naghdi (1969). Considering the changing between surface and volume energy in deformed bodies, Sih (1985) gave a surface/volume energy density theory to account for the mutually thermomechanical coupling effects. Such theory has already been applied to a host of problems and the predictions agreed with experiments (Sih and Tzou, 1986; Sih et al., 1987; Sih and Chao, 1989a, 1989b). Sluzalec (1992) proposed a coupled model to analyze the temperature change in elastic–plastic metals by using the concept of internal state variables.

As to the study of thermomechanical coupling effect in nonmetallic or cracked bodies, some theoretical and experimental researches were reported by Tauchert (1967), Tauchert and Afzal (1967), Sih and Tzou (1986), Tzou and Sih (1988), Pippan and Stuwe (1982), Yuan (1988, 1994) and Wu and Glockner (1996). Recently, Kinra and Bishop (1996) presented an approximate analysis of a Griffith crack in a specimen subjected to harmonic loading in modes I, II and III.

In experimental studies, the landmark works of Farren and Taylor (1925) and Taylor and Quinney (1934) demonstrated that nearly all of the hysteretic loss in elastic–plastic solids is converted into heat. All of the early experiments (Dillon, 1962b, 1966, among orthers) were performed with contacting measurement devices, such as thermocouples or thermistors. Non-contacting temperature measurement for single point by infrared detector was probably first investigated by Belgen (1967). Wilburn (1977) studied the profiles of temperature distribution during tensile test of steel SAE 4130 by using this technique. Thereafter, Mountain and Webber (1978) developed a scanning point detector system for full-field measurement. Using this technique, Pye and Adams (1981) monitored the fatigue damage and mapping of the stress field during cyclic mechanical testing. Huang et al. (1980, 1984) observed the energy change during standard tensile test and fatigue process of different types of steel. Gao and Yuan (1991) measured the temperature rise near the tip during crack propagation.

It is generally pointed out by experiments and simulation results of the thermomechanical coupling models mentioned above that during the initial elastic response the deformation causes cooling in uniaxial tension and heating in uniaxial compression, while pure torsion shows no temperature change for isotropic materials, and monotonous deformation in the inelastic region causes only self-heating.

The primary objective of this paper is threefold. First, the temperature fluctuation in an ABS specimen with prefabricated mesoscopic holes and/or mesocracks under plane stress is measured. Second, the cooling and heating phenomena observed in experiments are preliminarily and qualitatively explained, considering the microscopic and mesoscopic characteristics of deformation of polymers. Third, the heat converted from inelastic deformation is calculated from the local temperature field and compared with the external work.

2. Basic equations

Omitting the elaborate derivation, we list the basic equations controlling the thermomechanical state of a solid body subjected to external load and temperature changes (Allen, 1991).

The constitutive equation is assumed as:

$$\sigma_{ij} = \sigma_{ij}^0 + D_{ijkl}\left(\varepsilon_{kl} - \varepsilon_{kl}^1 - \beta_{kl}\theta\right), \tag{1}$$

where σ_{ij}^0 is the initial stress at zero strain and temperature change, D_{ijkl} is the elastic modulus tensor, ε_{ij} and ε_{kl}^1 are the strain tensor and the inelastic strain tensor respectively, β_{kl} is the thermal expansion tensor and $\theta = T - T_0$ is the difference between the instantaneous absolute temperature T and the reference temperature T_0.

The coupled heat conduction equation for anisotropic inelastic media:

$$(k_{ij}T_{,j})_{,i} = \rho c_v \dot{T} - \rho r + D_{ijkl}\beta_{kl}T\left(\dot{\varepsilon}_{ij} - \dot{\varepsilon}_{ij}^1\right) - \eta\sigma_{ij}\dot{\varepsilon}_{ij}^1, \tag{2}$$

where c_v is the specific heat at constant volume, $\eta \leq 1$ is a positive scalar function of inelastic deformation.

The entropy equation:

$$\rho T(s - s_0) = TD_{ijkl}\beta_{kl}\left(\varepsilon_{ij} - \varepsilon_{ij}^1\right) + \rho c_v\theta, \tag{3}$$

where s and s_0 represent the current and the initial entropy per unit mass respectively.

For an isotropic elastic material, Eqs. (2) and (3) can be simplified as

$$kT_{,ii} = \rho c_v \dot{T} - \rho r + (3\lambda + 2\mu)\beta T\dot{\varepsilon}_{kk} \tag{4}$$

and

$$\rho T(s - s_0) = T(3\lambda + 2\mu)\beta\varepsilon_{kk} + \rho c_v\theta. \tag{5}$$

Eq. (5) shows that the entropy change in an isotropic elastic material reflects the temperature change and the volumetric strain.

3. Experimental procedure

3.1. Specimen and material

Consider a thin flat specimen made of ABS, a typical thermoplastic copolymer which contain prefabricated defects. The dimensions of the specimen and the spatial distribution of the defects are shown in Fig. 1, in which $d = 5$ mm, $\alpha = 70^\circ$ and the specimen thickness $h = 4$ mm. The type and number of defects may be different in different specimen. The data for three different types of specimen are listed in Table 1. The physical properties of the tested material are listed in Table 2.

3.2. Test method

Infrared radiation occurs in any material when its temperature is above absolute zero. The power of infrared radiation is dependent on the temperature of the body. Therefore, the deformation-induced

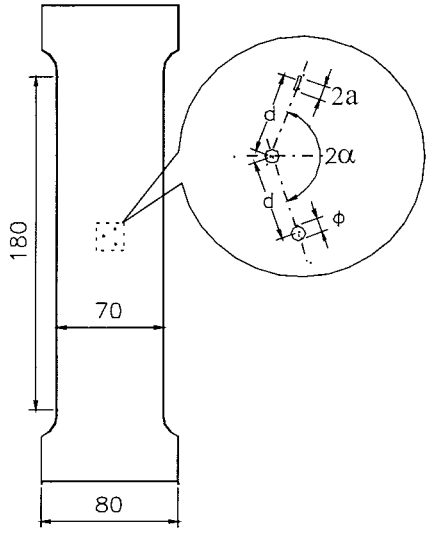

Fig. 1. Shape, dimensions and defect distribution of the tested specimen.

temperature fluctuation in materials can be recorded by using the infrared (IR) technique, whose features are real-time, quick and non-contacting to the specimen. In the present experiments, the temperature variation of the specimen due to thermal mechanical coupling was detected and recorded by using the IR technique.

Tests were carried out on an LST-50S type test machine which is an electrohydraulic servosystem. The specimen were loaded with a uniform displacement rate of $\dot{u} = 9.0$ mm/min at a room temperature of 15.2°C. A 6T61 type high sensitive infrared scanner (6T61IRS) was used to monitor and record the surface temperature changes in the area of the tested specimen where the defects are located. The working principle of this test system is shown in the block diagram of Fig. 2. It consists of the test machine, 6T61IRS, a digital/analog tape recorder (D/ATR), a four-channel tape recorder (FCTR), a dual channel spectrum analyzer (DCSA) and a microcomputer. The electric signals of the loads and

Table 1
Defect type and number in different specimen

Specimen type	Defect type	Number of prefabricated defects
I	mesoscopic hole ($\phi = 1.5$ mm)	2
II	mesoscopic hole ($\phi = 1.5$ mm)	3
III	mesoscopic crack ($2a = 1.5$ mm)	3

Table 2
Physical properties of ABS

Density	Tensile strength	Specific heat capacity	Thermal conductivity	Thermal linear expansion
1040 kg m^{-3}	48 ± 2.5 MPa	1406 J kg^{-1} K^{-1}	0.2–0.33 W m^{-1} K^{-1}	9.0×10^{-5} K^{-1}

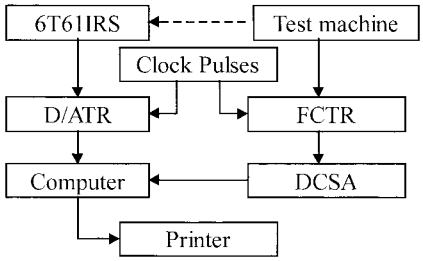

Fig. 2. Block diagram of test system.

displacements during testing, together with the clock pulses, were recorded by the FCTR, then converted into digital values via the DCSA, and finally input to a computer. Thus the load–displacement curves were obtained via the computer. The surface temperature of the specimen was detected and demarcated analogously with different colors. The analog signal of colors could also be digitized via the analog-to-digital converter unit of the D/ATR, and stored on the tape or a personal computer for subsequent analysis.

4. Experimental results and analyses

4.1. Local temperature field

The fluctuation of the surface temperature of the specimen was observed in the experiments. A typical picture of the local temperature field at a certain moment is shown in Fig. 3. Cooling of the specimen occurred in the initial elastic loading stage, which indicated that there was a certain endothermic excitation embedded in the materials. Stress whitening surrounding the defects was observed during further load increasing stage. At that moment, the stress and strain responses were already in the

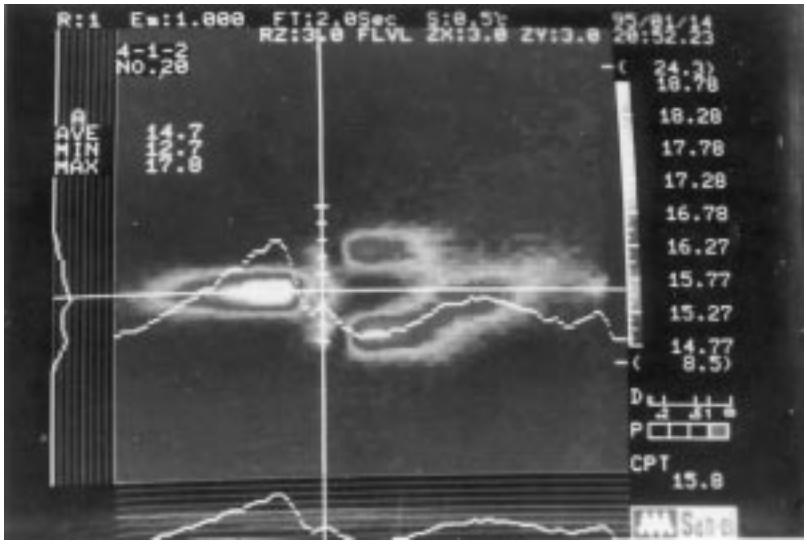

Fig. 3. A typical picture of the local temperature field.

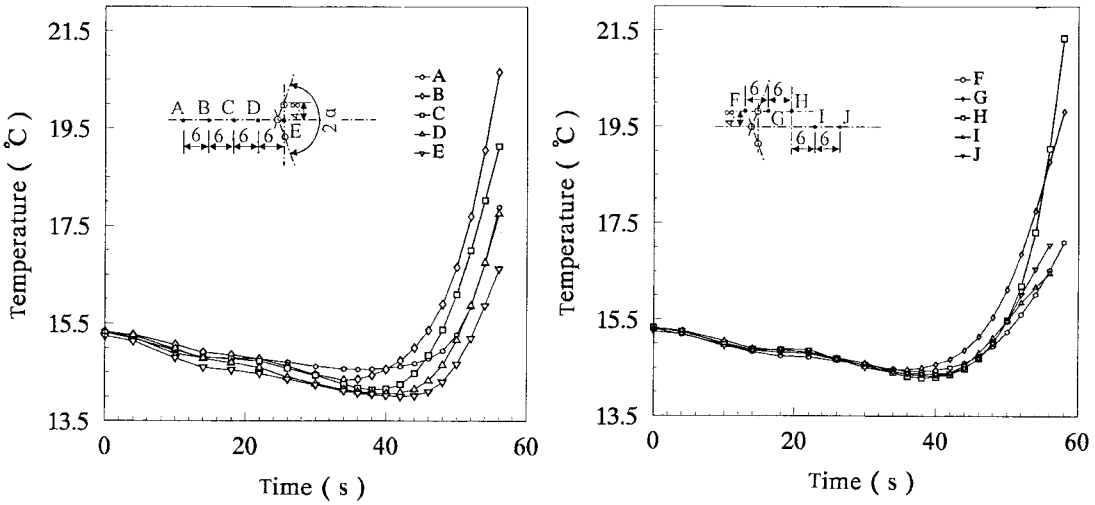

Fig. 4. The temperature history of ten points near defects in specimen II.

nonlinear range as the material was being permanently deformed. The local temperature returned to room condition and then rose steeply up to the macroscopic rupture of the specimen. Such phenomena of cooling and heating for ten spots (A, B, C,..., J) near the defects in specimen II are clearly exhibited by the curves in Fig. 4 which indicate that the maximum temperature drop was 1.3°C and the maximum temperature rise was approximately 6.0°C. The variation of the local temperature field near defects with the load for specimen II is shown in Fig. 5. During the elastic stage, the temperature drop is quite uniform over the entire surface of the specimen.

To understand the cause and mechanism of the cooling and heating phenomena, the microscopic and mesoscopic physical characteristics of the deformation of polymers should be summarized briefly.

The molecular chains of polymers are asymmetric in geometry. The ratio of the length to diameter of the chains may range from 100 to 10000. When a glassy polymer is subjected to external load, the molecules slide past each other and tend to uncoil to form an oriented structure in the direction of the principal stress. In fact, such orientation is the ordering process in which the molecules overcome the secondary (e.g. van der Waals) bonds and disentangle to align. It indicates the decrease of conformational entropy of the deformed polymer.

For simplicity, the glassy polymer is assumed to be initially isotropic. According to Eq. (5), in which $\varepsilon_{kk} > 0$ for uniaxial tension in the present experiments, during the elastic deformation, the decrease of the conformational entropy in material, that is $s-s_0 < 0$, will give

$$T < T_0; \tag{6}$$

Eq. (6) agrees well with the cooling phenomenon observed and indicates the grouping of heat sinks.

As the applied load increased, the orientational motion tended to reach the limit. For specimen II such a state first occurred in the defective area which had the high stress concentration at 34–36 sec. The local temperature of the material near the defects dropped down to a valley as shown in Fig. 4. During further loading, the molecular chains subjected to high stresses broke down, and the stresses were then redistributed to the adjacent chains. Thus the chain breakdown occurred concentratedly in a local area and accumulated to form microvoids. When the density of microvoids increased to a critical value, the microvoids expanded rapidly together to form craze (Kinloch and Young, 1983). The stress whitening observed resulted from the grouping of quite tiny but highly concentrated crazes. Crazes retain a

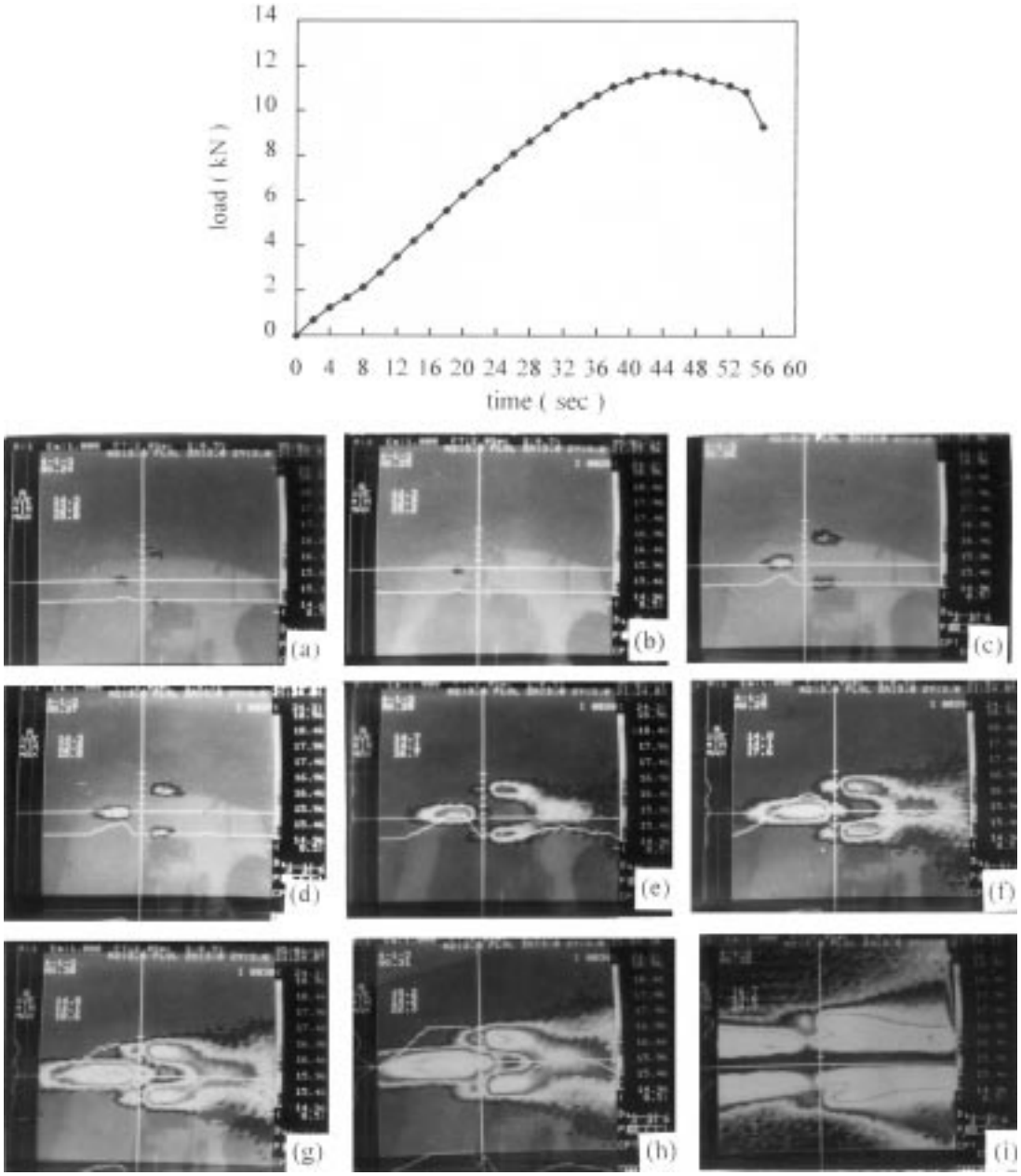

Fig. 5. Load history and photos of the local temperature field in specimen II under a constant displacement rate of 9.0 mm/min: (a) 40 s, (b) 42 s, (c) 44 s, (d) 46 s, (e) 48 s, (f) 50 s, (g) 52 s, (h) 54 s, (i) 56 s.

considerable strength because of the existence of craze matters. They expand by the meniscus instability mechanism and thicken by surface drawing mechanism in the direction perpendicular to the craze surfaces. Crazing is one of the important plastic deformation mechanisms in polymers.

Shear yielding, another important plastic deformation mechanism, was also observed in the experiments. The like-shear-lips were found by observing the fracture surfaces.

Both crazing and shear yielding imply that a plastic deformation zone came into being in the defective area. Most of the plastic deformation energy dissipated in the form of heat. Consequently the inner heat sources provided the heat generation to form the local temperature field, and gathered in the area near the corresponding defects. The heating stage corresponded to the non-linear range of load–displacement curve as shown in Fig. 5.

4.2. Heat generation

From an energy point of view, the energy absorbed in plastic deformation during defect evolution is converted into three parts: a small part of free elastic potential which can be released via elastic recovery; a little larger part of restraint potential stored in the deformed body and the major part of generated heat which forms the local temperature field.

Without considering the heat transfer between deformed body and its environment, at time τ during the defect evolution, the generated heat Q can be calculated from the temperature field as follows:

$$Q = \int_V \rho c_v \theta(\mathbf{x},\tau) \mathrm{d}V, \tag{7}$$

in which, $\mathbf{x}$ denotes the position vector. Generally, c_v and ρ are dependent on temperature. However they are taken to be constants in the following analysis since the temperature change is small. The isothermal surfaces are considered to be perpendicular to the surfaces of the thin plate specimen. Thus, Eq. (7) can be rewritten as

$$Q = \rho c_v h \sum_{i=1}^{n} (A_i - A_{i-1}) \theta_i, \tag{8}$$

where h denotes the thickness of the specimen, A_i and A_{i-1} are the areas encircled by two adjacent isothermal lines, respectively. The area between two such isothermal lines is considered to be isothermal in which the temperature rise is θ_i.

If the areas, S_i, encircled by isothermal lines with regular temperature intervals (say θ_0) are determined, the generated heat revealed in the temperature field can be expressed by

$$Q = \rho c_v h \theta_0 \sum_{i=1}^{n} S_i. \tag{9}$$

Taking $\theta_0 = 0.25^\circ$C in the data processing, the generated heat during deformation of specimen I, II and III was calculated from Eq. (9), in which S_i could be determined by a boundary self-tracking procedure programmed by the first author of this paper. The generated heat was also compared with the external work, which was calculated from the load–displacement curve.

Fig. 6(a) shows that the maximum generated heat was 24.3 J(oule), while the external work was 56.35 J in specimen I. In specimen II, the maximum generated heat was 28.2 J while the external work was 63.74 J [Fig. 6(b)]. In specimen III, the maximum generated heat was 27.08 J while the external work was 38.7 [Fig. 6(c)]. It is shown in the present experiments that the heat generated in specimen with mesoscopic holes approximated to 25–44 percent of the external work, while that in specimens with mesocracks approximated to 45–70 percent of the external work. Such results indicate that a considerable part of the external work is dissipated in irreversible deformation and converted into heat.

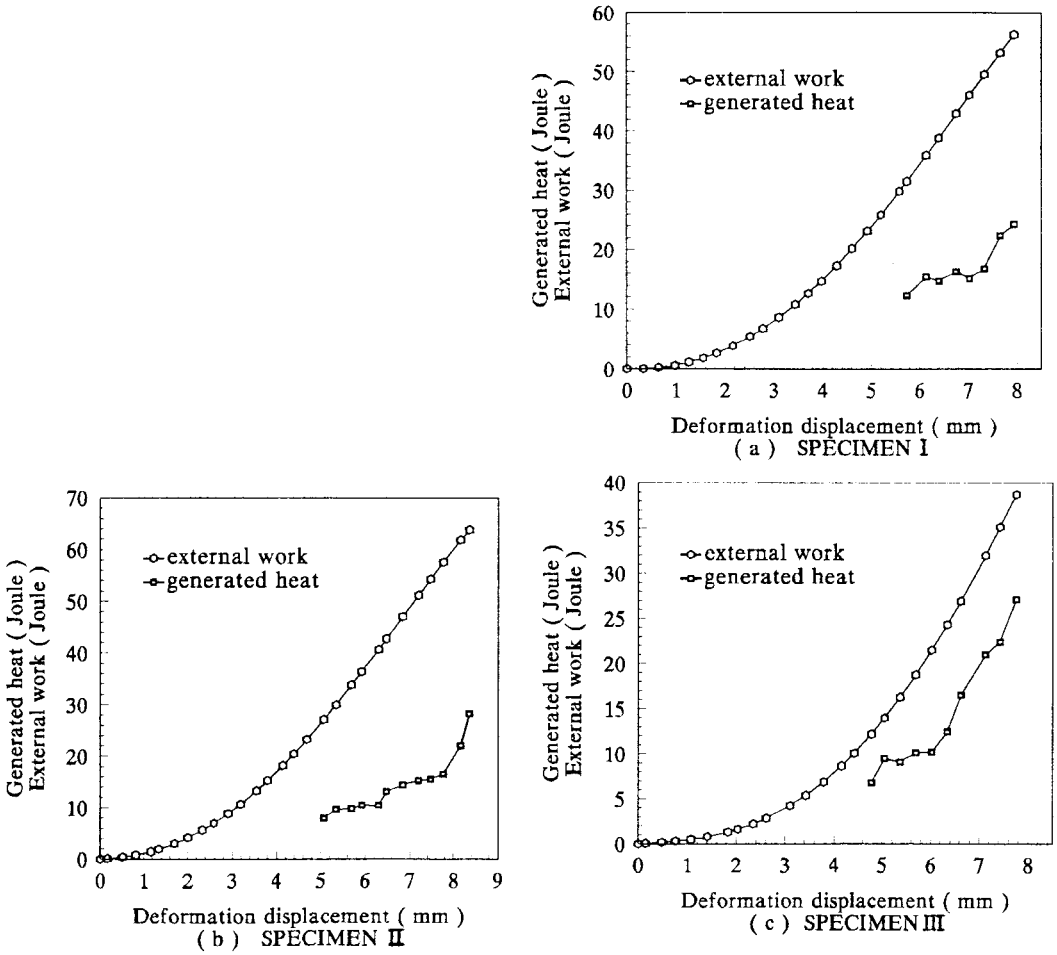

Fig. 6. Variations of generated heat and external work with displacement in specimen I, II and III.

5. Concluding remarks

The initiation and evolution of the local temperature field in a glassy copolymer with prefabricated defects were measured by infrared photography. The cooling of specimen surfaces during the initial elastic deformation and the heating in the inelastic deformation process were observed in the present experiments. Based on the deformation characteristics of glassy polymers, this paper explained the cooling and heating phenomena in deformed specimens, at both the microscopic and mesoscopic levels, preliminarily and quantitatively. By considering the isothermal surfaces to be perpendicular to the specimen surfaces, the heat revealed in the local temperature field was calculated. It approximated to 25–44 percent of the external work in specimens with mesoscopic holes and to 45–70 percent in specimens with mesocracks.

Acknowledgements

The research reported was supported by the National Natural Science Foundation of China (NSFC-19632030) and LNM of Institute of Mechanics, CAS. The authors are also grateful to Professor R. Wang for his useful discussions and suggestions.

References

Allen, D.H., 1985. A prediction of heat generation in a thermoviscoplastic uniaxial bar. Int. J Solids Structures 21 (4), 325–342.
Allen, D.H., 1986. Predicted axial temperature gradient in a viscoplastic uniaxial bar due to thermomechanical coupling. Int. J. Num. Methods Eng. 23 (5), 903–917.
Allen, D.H., 1991. Thermomechanical coupling in inelastic solids. Appl. Mech. Rev. 44 (8), 361–373.
Audoly, S., Paglietti, A., 1985. Thermo-mechanic coupling in dynamic plasticity during uniaxial tests. Engng Fracture Mech. 21 (4), 653–661.
Belgen, M.H., 1967. Structural stress measurement with an infrared radiometer. ISA Trans. 6, 49–53.
Cernocky, E.P., Krempl, E., 1980. A theory of thermoviscoplasticity based on infinitesimal total strain. Int. J. Solids Structures 16, 723–741.
Christensen, R.M., 1967. Linear non-isothermal viscoelastic solids. Acta Mechanica 3 (1), 1–12.
Christensen, R.M., 1971. Theory of Viscoelasticity, an Introduction. Academic Press, New York.
Compton, K.T., Webster, D.B., 1915. Temperature changes accompanying the adiabatic compression of steel. Phys. Rev. V, 159–166.
Crochet, M.I., Naghdi, P.M., 1969. A class of simple solids with fading memory. Int. J. Eng. Sci. 7, 1173–1198.
Dillon Jr., O.W., 1962a. A nonlinear thermoelastic theory. J. Mech. Phys. Solids 10, 123–131.
Dillon Jr., O.W., 1962b. An experimental study of the heat generated during torsional oscillations. J. Mech. Phys. Solids 10, 235–244.
Dillon Jr., O.W., 1966. The heat generated during the torsional oscillations of copper tubes. Int. J. Solids Structures 2, 181–204.
Duhamel, J.M.C., 1837. Second memoire sur les phenomenes thermo-mecaniques. J. de l'Ecole Polytechnique 15 (25), 1–57.
Farren, W.S., Taylor, G.I., 1925. The heat developed during plastic extension of metals. Proc. Roy. Soc. A 107, 422–451.
Gao, Y.X., Yuan, L.W., 1991. Thermodynamical coupled relation of dissipative rheological solid. In: Proc. China–Japan Int. Conf. Rheology. Peking University Press, Beijing, pp. 338–342.
Ghoneim, H., 1986. Thermoviscoplasticity by finite element: dynamic loading a thick-walled cylinder. J. Thermal Stresses 9, 345–358.
Ghoneim, H., Matsuoka, S., 1987. Thermoviscoplasticity by finite element: tensile and compression test. Int. J. Solids Structures 23 (8), 1133–1143.
Ghoneim, H., 1990. Analysis and applications of a coupled thermoviscoplasticity theory. J. Appl. Mech. 57, 828–835.
Huang, Y., Xu, J., Shih, C.H., 1980. Application of infrared technique to research on tensile test. Materials Evaluation 38, 71–79.
Huang, Y., Li, S.X., Lin, X.R., Shih, C.H., 1984. Using the method of infrared sensing for monitoring fatigue process of materials. Materials Evaluation 42, 1020–1024.
Kinloch, A.J., Young, R.J., 1983. Fracture Behaviour of Polymers. Applied Science Publishers, London and New York.
Kinra, V.K., Bishop, J.E., 1996. Elastothermodynamic analysis of a Griffith crack. J. Mech. Phys. Solids 44 (8), 1305–1336.
Mountain, D.S., Webber, J.M.B., 1978. Stress pattern analysis by thermal emission (SPATE). Proc. Soc. Photo-Opt. Inst. Eng. 164, 189–196.
Paglietti, A., 1982. Interaction of heat production, strain rate and stress power in a plastically deforming body under tensile test. In: Research in Structural and Solid Mechanics, pp. 113–127 NASA Conference Publ. No. 2245.
Pippan, R., Stuwe, H.P., 1982. The temperature field surrounding the fatigue crack tip. In: Maurer, K.L., Matzer, F.E. (Eds.), Proc. of the 4th E.C.F, vol. 2, pp. 457–459.
Prigogine, I., 1962. Introduction to Nonequilibrium Thermodynamics. Wiley–Interscience, New York.
Pye, C.J., Adams, R.D., 1981. Detection of damage in fible reinforced plastics using thermal fields generated during resonant vibration. NDT International 14, 111–119.
Schapery, R.A., 1969. On the characterization of nonlinear viscoelastic materials. Poly. Eng. Sci. 9, 295–310.
Sih, G.C., 1985. Mechanics and physics of energy density theory. Theoret. Appl. Fracture Mech 4 (3), 157–173.
Sih, G.C., Tzou, D.Y., 1986. Heating predicted by cooling ahead of crack: macrodamage free zone. Theoret. Appl. Fracture Mech. 6 (2), 103–111.

Sih, G.C., Lieu, F.L., Chao, C.K., 1987. Thermal/mechanical damage of 6061-T6 aluminium tensile specimen. Theoret. Appl. Fracture Mech. 7 (2), 67–78.

Sih, G.C., Chao, C.K., 1989a. Scaling of size/time/temperature, Part I: Progressive damage in uniaxial tensile specimen. Theoret. Appl. Fracture Mech. 12 (2), 93–108.

Sih, G.C., Chao, C.K., 1989b. Scaling of size/time/temperature, Part II: Progressive damage in uniaxial compressive specimen. Theoret. Appl. Fracture Mech. 12 (2), 109–119.

Sluzalec, A., 1992. Temperature rise in elastic–plastic metal. Computer Methods in Applied Mechanics and Engineering 96, 293–302.

Tauchert, T.R., 1967. The temperature generated during torsional oscillations of polyethylene rods. Int. J. Eng. Sci. 5, 353–365.

Tauchert, T.R., Afzal, S.M., 1967. Heat generated during torsional oscillations of polymethyl–methacrylate tubes. J. Appl. Phys. 38, 4568–4572.

Taylor, G.I., Quinney, H., 1934. The latent energy rmaining in a metal after cold working. Proc. Royal Soc. 143, 307–326.

Thomson, W., 1853. Dynamical theory of heat with numerical results deduced from Mr. Joule's equivalent of a thermal unit and M. Regnault's observation on steam. Trans. Royal Soc. Edinburgh 20, 161–283.

Tzou, D.Y., Sih, G.C., 1988. Thermal/mechanical interaction of subcritical crack growth in tensile specimen. Theoret. Appl. Fracture Mech. 10 (1), 59–72.

Wilburn, D.K., 1977. Temperature profiles observed in tensile specimens during physical test. Materials Evaluation 35 (3), 28–31.

Wu, Z., Glockner, P.G., 1996. Thermo-mechanical coupling applied to plastics. Int. J. Solids Structures 33 (29), 4431–4448.

Yuan, L.W., 1988. Theoretical and experimental research on nonlinear rheological fracture for polymer solids. In: Proc. Xth Int. Cong. Rheology, vol. 2. Monash University Printing Service, Sydney, pp. 389–391.

Yuan, L.W., 1994. Rheology of Defect Body. National Defense Industry Press, Beijing (in Chinese).